Effects of simvastatin-loaded PLGA microspheres on treatment of rats with intervertebral disk degeneration and on 6-K-PGF1α and HIF-1α

KAI ZHU[1,2], FUTING ZHAO[3], YANHUA YANG[4] and WEIDONG MU[1]

[1]Department of Traumatic Orthopedics, Shandong Provincial Hospital Affiliated to Shandong University, Jinan, Shandong 250021; [2]Department of Spine Surgery, Binzhou Medical University Hospital, Binzhou, Shandong 256603; [3]Department of Orthopedics, Qingyun County People's Hospital, Dezhou, Shandong 253700; [4]Department of Pathology, Qingdao Municipal Hospital, Qingdao, Shandong 266011, P.R. China

Received September 6, 2019; Accepted November 1, 2019

DOI: 10.3892/etm.2019.8267

Abstract. Effects of simvastatin-loaded PLGA sustained release microspheres on the treatment of rats with intervertebral disk degeneration (IVDD) and on 6-keto-prostaglandin F1α (6-K-PGF1α) and hypoxia inducible factor-1α (HIF-1α) were investigated. Eighty female rats were selected and randomized into a model group (modeled for IVDD), a treatment group (modeled and treated with simvastatin-loaded PLGA sustained release microspheres), a sham operation group (only operated without excision), and a control group (not treated) (n=20 each). After modeling, 6-K-PGF1α and HIF-1α in the peripheral blood of the rats were, respectively, detected before simvastatin injection (T0), at 2 weeks (T1) and 4 weeks (T2) after simvastatin injection. The bone mineral density (BMD) of L_5 and L_6 was detected by X-ray. The trabecular thickness, number, and separation of the vertebral body were detected. Changes in the sagittal T2-weighted signal of intervertebral disc nucleus pulposus were detected by MRI. There were no differences between the control and sham operation groups in the indices (P>0.050). Compared with those in the model group during the treatment, BMD, 6-K-PGF1α, HIF-1α, and trabecular number in the treatment group significantly increased (P<0.050), while the trabecular separation significantly decreased (P<0.050). The sagittal T2-weighted MRI signal in the model group was the lowest between the four groups (P<0.050). Simvastatin-loaded PLGA sustained release microspheres can improve the BMD of the vertebral body and increase the contents of 6-K-PGF1α and HIF-1α in the treatment of rats with IVDD, so they are important for the clinical treatment of the disease.

Correspondence to: Dr Weidong Mu, Department of Traumatic Orthopedics, Shandong Provincial Hospital Affiliated to Shandong University, 324 Jingwuweiqi Road, Jinan, Shandong 250021, P.R. China
E-mail: m9u11q@163.com

Key words: simvastatin, PLGA, 6-K-PGF1α, HIF-1α, bone mineral density

Introduction

Intervertebral disk degeneration (IVDD) that has unclear specific pathogenesis is mainly manifested as lower back pain and acute nerve root pain of lower extremity (1). Data show that the disease is extremely common worldwide. More than 80% of adults may suffer from different degrees of the degeneration (2), and the degree greatly increases among the middle-aged and elderly patients (3). As the population ages, the risk of IVDD is increasing (4). The disease can easily cause a series of lumbar diseases such as intervertebral disc herniation and degenerative disc diseases, even impaired walking and lower limb paralysis (5). According to statistics, over 40% of the lumbar diseases are mainly caused by it (6). Currently, the treatment of IVDD is based on conservative treatment or surgical operation, but both only relieve symptoms and cannot completely cure the disease (7).

Worldwide researchers are exploring new therapeutic methods for increasingly serious IVDD. With the deepening of research, increasing number of reports point out that cytobiology may be crucial to treat the disease in the future (8,9). Bone morphogenetic protein (BMP) plays a pivotal role in affecting the synthesis of intervertebral disc extracellular matrix. In addition to rebuilding intervertebral disc function, its upregulation promotes the expression of type II collagen and glycoprotein in normal nucleus pulposus cells and in the extracellular matrix of degenerated nucleus pulposus (10). Statin simvastatin is a hydroxymethylglutaryl coenzyme A (HMG-CoA) reductase. Its pharmacological mechanism has been proven to upregulate BMP-2 in nucleus pulposus cells through the mevalonic acid pathway (11), but its clinical application is limited due to its water insolubility (12). As a drug sustained-release system commonly used in clinical practice, polylactic-co-glycolic acid (PLGA) can specifically administer drugs, improve drug stability, and control drug release, so it has been applied in the treatment of many diseases (13,14). It is speculated that simvastatin-loaded PLGA sustained release

microspheres can cure IVDD, which remains uncertain due to lack of relevant research support. Therefore, in this study, a rat model of IVDD was established, and the treatment with simvastatin-loaded PLGA microspheres was observed, and prostaglandin markers 6-keto-prostaglandin F1α (6-K-PGF1α) and hypoxia inducible factor-1α (HIF-1α) were detected to analyze the therapeutic value of simvastatin for the disease.

Materials and methods

Animal data. Eighty 3-month-old Sragues-Dawley (SD) female healthy rats, weighting 210±20 g, were purchased from Beijing Vital River Laboratory Animal Technology Co., Ltd., with a certificate number of SCXK (Beijing) 2016-0011. They were normally fed and housed in lighted cages (5 rats each), with the temperature of 29±2˚C and the humidity of 40-50%.

Methods

Preparation of simvastatin-loaded PLGA. PLGA and simvastatin were dissolved in methylene chloride at 10:3.3, shaken and well mixed, and then added with distilled water (200 μl) for ultrasonic mixing. Next, the mixture was slowly added with 5% polyvinyl alcohol aqueous solution (100 ml) for ultrasonic mixing. Then, the mixture was added with 0.3% polyvinyl alcohol aqueous solution (50 ml), stirred, well mixed, and then allowed to stand at room temperature for 12 h. After the organic solution was removed, the mixture was frozen and dried for 48 h.

Detection of encapsulation efficiency and drug loading of microspheres. Microspheres (5 mg) were selected and prepared into an ethanol solution (100 ml), to measure the optical density (238 nm) of the solution with ethanol as a blank control. The content of simvastatin in the microspheres was calculated according to the standard curve. Encapsulation efficiency = the total amount of simvastatin/the total amount of microspheres x100%. Drug loading = actual drug loading/theoretical drug loading x100%. The release curve of simvastatin was plotted according to the cumulative release.

Modeling method. All rats were divided into four groups (n=20 each) based on random number table. Rats in the model and treatment groups were modeled for IVDD, with the method described by Chen *et al* (15). After the rats were intraperitoneally injected with 2% pentobarbital sodium (40 mg/kg) for anesthesia, the morphology was observed. They were determined to enter deep anesthesia if they had disappearing responses to skin pain, relaxing muscles, and disappearing responses to eye and face irritation, as well as smooth breathing. Next, the rat chest was incised to expose the lower segment of the thoracic vertebra, and the upper segment of the lumbar vertebra and the sacrum. All lumbar spinous processes, supraspinous ligaments, lumbar segment of interspinous ligaments, and posterior outer 1/2 of lumbar facet joints on both sides were removed. Subsequently, deep fascia and skin were sutured, while erector spinae muscles were not sutured, and then bilateral ovaries were removed via ventral approach. X-ray fluoroscopy was conducted to determine whether the modeling was successful. Rats in the sham operation group were anesthetized. After that, their chest was incised to expose the lower segment of the thoracic vertebra, and the upper segment of the lumbar vertebra and the sacrum. Finally, the incision was sutured. Rats in the control group were not treated. Rats in the treatment group were treated with simvastatin-loaded PLGA microspheres, and injected with normal saline (2 μl) at 5 mg/ml. Rats in the model group were injected with the same dose of normal saline.

Outcome measures. After modeling, 5 rats in each group were sacrificed by cervical dislocation under anesthesia before simvastatin injection (T0), at 2 weeks (T1) and 4 weeks (T2) after simvastatin injection, respectively. Enzyme-linked immunosorbent assay (ELISA) was used to detect the concentrations of 6-K-PGF1α (the kit was purchased from Shanghai Hengfei Biotechnology Co., Ltd.; CSB-E14411r-1) and HIF-1α (the kit was purchased from Shanghai Qiaoyu Industrial Co., Ltd.; QY-Q11659) in the peripheral blood of rats. The lumbar vertebrae $L_{5\text{-}6}$ of the rats were obtained, and the bone mineral density (BMD) of L_5 and L_6 was detected by X-ray. After the injection, CT was carried out to scan the vertebral body of the rats and reconstruct the scanned area in three dimensions. The trabecular thickness, number, and separation of the vertebral body were detected. Changes in the sagittal T2-weighted signal were detected by MRI to detect the intervertebral disc nucleus pulposus of the rats.

Evaluation program of humane endpoint. Weight loss: The rats lost 15-20% of the original body weight within 2 days, or they had no sustained weight gain in growth period, or they had cachexia and sustained muscle consumption without weight monitoring. Weakness: The rats were unable to feed and drink on their own, and they were unable to stand for 24 h or they could stand with extreme efforts. The recovery period after anesthesia was excluded, and then whether they were weak due to diseases, experiments, or other factors was evaluated. Organ infection: The rats had abnormal physical indices and blood test values, but no good response to drug treatment; additionally, the disease progressed to a systemic disease. Respiratory system: The rats had severe respiratory tract infection, dyspnea, or cyanosis. Circulatory system: The rats had severe anemia, uncontrollable hemorrhage (PVC <15%), or jaundice. Nervous system: The rats had abnormal central nervous system reactions (convulsion, trembling, paralysis, and torticollis) or uncontrollable pain. Others: The rats had persistent self-mutilation behavior, non-healing wounds, diseases that seriously affected eating and drinking water, advanced infectious diseases, persistent hypothermia, significant functional damage to organs and facial features, or behaviors and physiological phenomena when they suffered from distress and pain. The study was approved by the Ethics Committee of Shandong Provincial Hospital Affiliated to Shandong University.

Death determination. The rats were laid on one side and they were determined to be dead if they could not turn over to a normal posture within 30 sec.

Statistical analysis. In this study, SPSS 24.0 (Shanghai Yuchuang Network Technology Co., Ltd.) was used to statistically analyze the results. GraphPad 8 (Softhead Inc.) was used to plot figures. Enumeration data were expressed by rate,

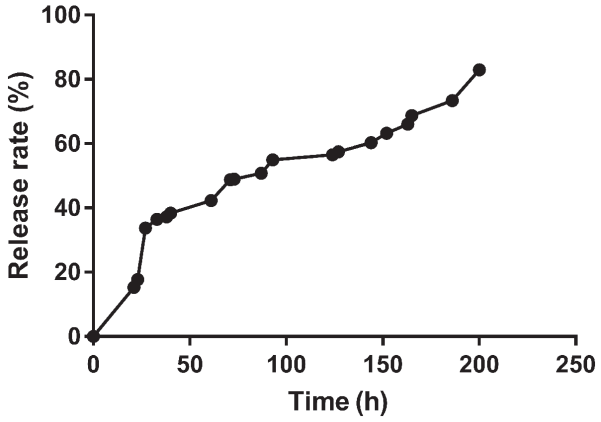

Figure 1. A microsphere release curve.

and Chi-square test was used for comparison between groups. Measurement data were expressed as mean ± standard deviation, and t-test was used for comparison between groups. Repeated measures analysis of variance and Bonferroni post hoc test were used for comparison between multiple time-points. P<0.050 indicated a statistically significant difference.

Results

Simvastatin-loaded PLGA sustained release microspheres. The drug loading of the microspheres was 22.85±1.85%, and the encapsulation efficiency was 91.12±2.78%, and the cumulative release was >80%, which indicated successful preparation (Fig. 1).

Modeling results. Of the 40 rats modeled, 20 in the treatment group and 19 in the model group were successfully modeled, with a success rate of 97.5%.

Detection results of BMD. At T0, there was no significant difference in BMD between the treatment and model groups (P>0.050), and between the sham operation and control groups (P>0.050). BMD in the model and treatment groups was lower than that in the sham operation and control groups (P<0.050). At T1, there was no significant difference between the sham operation and control groups (P>0.050). BMD in the two groups was higher than that in the model and treatment groups, while BMD in the treatment group was higher than that in the model group (P<0.050). At T2, there was no significant difference between the sham operation, control, and treatment groups (P>0.050), and BMD in the three groups was higher than that in the model group (P<0.050). There was no difference in BMD at T0, T1 and T2 between the sham operation, control, and model groups (P>0.050). BMD in the treatment group was the lowest at T0 and the highest at T2 (P<0.050) (Fig. 2).

6-K-PGF1α and HIF-1α. At T0, there were no differences in 6-K-PGF1α and HIF-1α between the control and sham operation groups (P>0.050), but there were differences between the model and treatment groups (P>0.050). The two indices in the control and sham operation groups were higher than those in

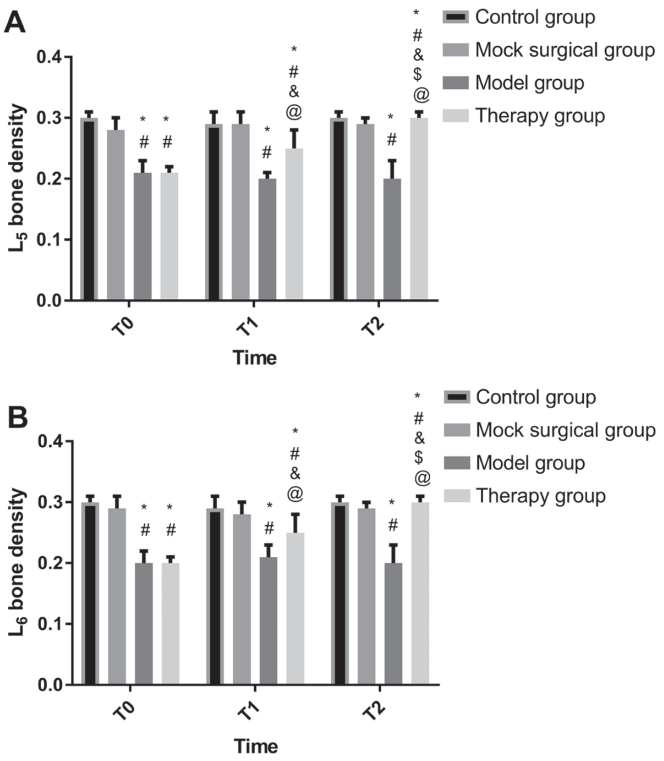

Figure 2. Detection results of BMD. (A) Comparison of the BMD of L_5 vertebral body between the four groups. (B) Comparison of the BMD of L_6 vertebral body between the four groups. *P<0.050 when compared with BMD in the control group at the same time-point; #P<0.050 when compared with BMD in the sham operation group at the same time-point; &P<0.050 when compared with BMD in the model group at the same time-point; @ P<0.050 when compared with BMD at T0 in the same group; $P<0.050 when compared with BMD at T1 in the same group.

the model and treatment groups (P<0.050). At T1 and T2, there were no differences between the control and sham operation groups (P>0.050). The two indices in the two groups were higher than those in the treatment and model groups (P<0.050), while those in the treatment group were higher than those in the model group (P<0.050). There were no differences in the indices at T0, T1 and T2 between the control and sham operation groups (P<0.050). The indices in the model group were the highest at T0 and the lowest at T2 (P<0.050). The indices in the treatment group were the lowest at T0 and the highest at T2 (P<0.050) (Fig. 3).

CT results. There was no difference in the trabecular thickness between the four groups (P>0.050), and in the trabecular number and separation between the control and sham operation groups (P>0.050). The trabecular number in the control and sham operation groups was higher than that in the treatment and model groups, and that in the model group was the lowest (P<0.050). The trabecular separation in the two groups was lower than that in the treatment and model groups, and that in the model group was the highest (P<0.050) (Table I).

MRI results. After 8-week injection, there was no difference in the sagittal T2-weighted MRI signal of the intervertebral disc nucleus pulposus between the control and sham operation groups (P>0.050). The signal in the two groups was higher

Table I. Comparison of CT results.

	Control	Sham operation group	Model group	Treatment group	F-value	P-value
Trabecular thickness (μm)	105.52±4.28	101.52±3.15	103.62±3.42	103.57±4.16	0.933	0.448
Trabecular number (mm)	2.34±0.42	2.28±0.39	1.42±0.24[a,b]	1.83±0.25[a-c]	8.249	0.002
Trabecular separation (μm)	250.62±28.63	262.61±30.57	368.45±32.65[a,b]	316.74±25.61[a-c]	16.880	<0.001

[a]P<0.050 when compared with that in the control group; [b]P<0.050 when compared with that in the sham operation group; [c]P<0.050 when compared with that in the model group.

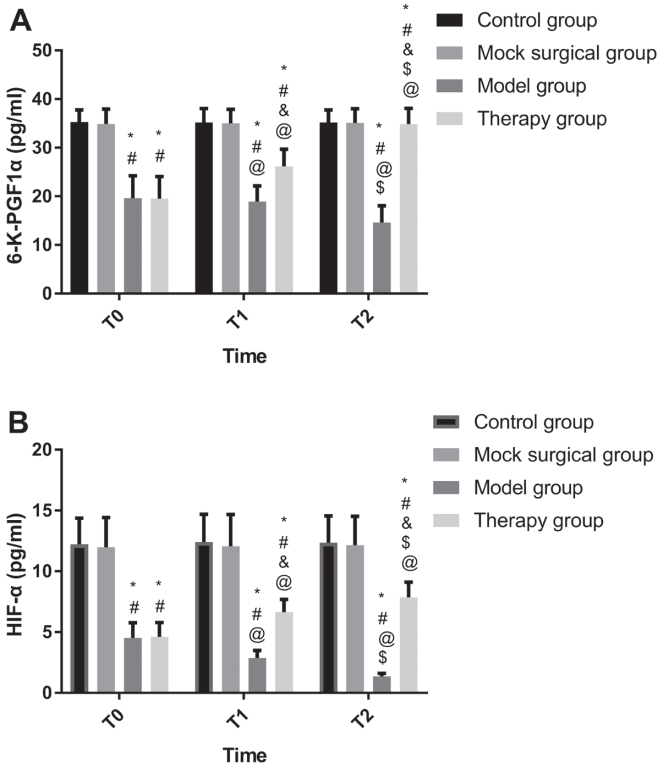

Figure 3. Detection results of 6-K-PGF1α and HIF-1α. (A) Comparison of 6-K-PGF1α between the four groups. (B) Comparison of HIF-1α between the four groups. *P<0.050 when compared with that in the control group at the same time-point; #P<0.050 when compared with that in the sham operation group at the same time-point; &P<0.050 when compared with that in the model group at the same time-point; $P<0.050 when compared with that at T0 in the same group; @P<0.050 when compared with that at T1 in the same group.

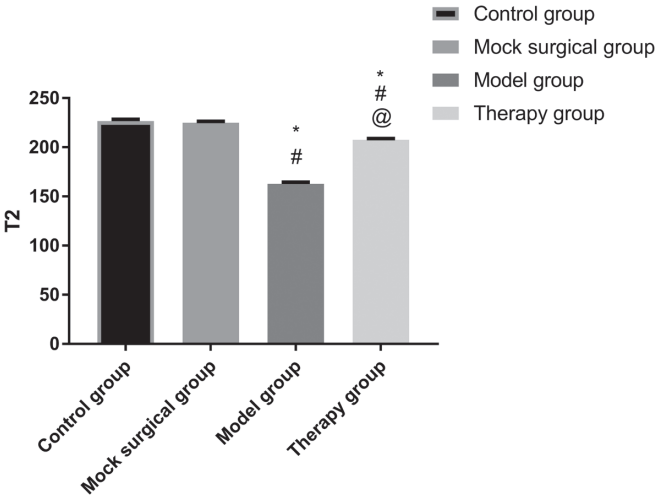

Figure 4. Comparison of sagittal T2-weighted MRI signal of intervertebral disc nucleus pulposus. *P<0.050 when compared with that in the control group; #P<0.050 when compared with that in the sham operation group; @P<0.050 when compared with that in the model group.

than that in the model and treatment groups (P<0.050), and that in the model group was the lowest (Fig. 4).

Discussion

IVDD is a very common chronic disease around the world with a high incidence and great harm, so it has long been a major research project in clinical practice (16). The effect of simvastatin on IVDD has been unanimously agreed, it improves bone quality by promoting the aggregation of type II collagen. However, it has not yet been widely used in clinical practice due to its extremely high limitation in human body (17). In this study, the effects of simvastatin-loaded PLGA microspheres on treating rats with IVDD were observed, to analyze the effective scheme of simvastatin in the treatment. In addition, 6-K-PGF1α and HIF-1α in the rats were detected to preliminarily analyze the influencing mechanism of simvastatin, which is of great significance for the clinical treatment of the disease in the future.

In this study, BMD in the treatment group was significantly higher than that in the model group after treatment, but partial BMD was not significantly different from that in the control group at T2. This confirms the important role of simvastatin in the bone tissue and the feasibility of treating IVDD with simvastatin-loaded PLGA sustained release microspheres, which was also proved by comparing the trabecular number, the trabecular separation, and the sagittal T2-weighted MRI signal between the four groups. Organic polymer material PLGA has good biodegradability, compatibility, non-irritant, and non-immunogenicity, so it has a great application prospect in clinical practice (18). PLGA was chosen as the sustained-release material of simvastatin, because its excellent drug loading, encapsulation efficiency, and release ensure its stable concentration for homeostasis during the action of simvastatin on IVDD. Many studies have confirmed that simvastatin mainly affects the intervertebral disc by upregulating BMP-2 (19,20), which was therefore not repeated here. According to the detection, 6-K-PGF1α and

HIF-1α at T0 in the treatment and model groups were lower than those in the control and sham operation groups, while the two indices in the treatment group significantly increased at T1 and T2, and were higher than those in the control and sham operation groups at T2. These findings suggest that simvastatin has a significant effect on 6-K-PGF1α and HIF-1α. Prostaglandin I_2 (PGI_2), a substance reflecting bioactivity and produced by arachidonic acid metabolism, dilates blood vessels and controls platelet aggregation (21). In human body, it is quickly hydrolyzed into inactive 6-K-PGF1α and maintains blood circulation (22). Fan *et al* (23) investigated the role of 6-K-PGF1α in hyperlipidemia and found that it is important for the formation of thrombosis. Although the pathogenesis of IVDD is not yet clear, previous studies have shown that the number of vascular buds in cartilage endplate decreases during pathogenesis, so hemodynamic abnormality may be a pathogenic factor for the disease (24). The significant effect of 6-K-PGF1α on hemodynamics may also be a mechanism of simvastatin in the treatment of IVDD. It is speculated that simvastatin may play an antithrombotic role by increasing the content of 6-K-PGF1α, so as to enhance the hemodynamics of patient tissues, and then protect and improve the integrity of bone tissues. 6-K-PGF1α usually functions in human body through coordinating with thromboxane A_2 (TXA_2). In this study, TXA_2 in each group was not detected, but it is a research emphasis in the future. As an important cytokine that makes tissues and cells adapt rapidly to low oxygen environment, HIF-1α promotes the generation of vascular endothelial growth factor (VEGF) and glucose receptor, and regulates cell apoptosis and differentiation (25). Lumbar intervertebral disc cells have been in a low oxygen microenvironment for a long time due to the aging of the body. At this time, HIF-1α is activated, which accelerates the synthesis of VEGF and protein (26). The increase in HIF-1α after simvastatin injection is possibly because the upregulation of VEGF expression promotes cardiovascular formation in the intervertebral disc tissue, thus delaying the progression of IVDD. Additionally, studies have confirmed the close correlations of 6-K-PGF1α and HIF-1α with BMP-2 (27,28). However, it is also possible that simvastatin regulates 6-K-PGF1α and HIF-1α through BMP-2 and then affects IVDD, which needs further confirmation.

This study has deficiencies due to the limited experimental conditions. For example, because of the differences between animal models and human beings, the concentration of simvastatin should be further confirmed, and the drug resistance of humans should be considered.

In conclusion, simvastatin-loaded PLGA sustained release microspheres can improve the BMD of the vertebral body and increase the contents of 6-K-PGF1α and HIF-1α in the treatment of rats with IVDD, so they are important for the clinical treatment of the disease.

Acknowledgements

Not applicable.

Funding

No funding was received.

Availability of data and materials

The datasets used and/or analyzed during the current study are available from the corresponding author on reasonable request.

Authors' contributions

ZK wrote the manuscript. ZK and ZF conceived and designed the study. ZF and YY were responsible for the collection and analysis of the experimental data. ZK and MW interpreted the data and drafted the manuscript. ZK and YY revised the manuscript critically for important intellectual content. All authors read and approved the final manuscript.

Ethics approval and consent to participate

The study was approved by the Ethics Committee of Shandong Provincial Hospital Affiliated to Shandong University, China.

Patient consent for publication

Not applicable.

Competing interests

The authors declare that they have no competing interests.

References

1. Feng C, Liu H, Yang M, Zhang Y, Huang B and Zhou Y: Disc cell senescence in intervertebral disc degeneration: Causes and molecular pathways. Cell Cycle 15: 1674-1684, 2016.
2. Feng Y, Egan B and Wang J: Genetic factors in intervertebral disc degeneration. Genes Dis 3: 178-185, 2016.
3. Wang F, Cai F, Shi R, Wang XH and Wu XT: Aging and age related stresses: A senescence mechanism of intervertebral disc degeneration. Osteoarthritis Cartilage 24: 398-408, 2016.
4. Zhang F, Zhao X, Shen H and Zhang C: Molecular mechanisms of cell death in intervertebral disc degeneration (Review). Int J Mol Med 37: 1439-1448, 2016.
5. Sun D, Liu P, Cheng J, Ma Z, Liu J and Qin T: Correlation between intervertebral disc degeneration, paraspinal muscle atrophy, and lumbar facet joints degeneration in patients with lumbar disc herniation. BMC Musculoskelet Disord 18: 167, 2017.
6. Corniola MV, Stienen MN, Joswig H, Smoll NR, Schaller K, Hildebrandt G and Gautschi OP: Correlation of pain, functional impairment, and health-related quality of life with radiological grading scales of lumbar degenerative disc disease. Acta Neurochir (Wien) 158: 499-505, 2016.
7. Zeckser J, Wolff M, Tucker J and Goodwin J: Multipotent mesenchymal stem cell treatment for discogenic low back pain and disc degeneration. Stem Cells Int 2016: 3908389, 2016.
8. Sakai D and Schol J: Cell therapy for intervertebral disc repair: Clinical perspective. J Orthop Translat 9: 8-18, 2017.
9. Chen K, Lv X, Li W, Yu F, Lin J, Ma J and Xiao D: Autophagy is a protective response to the oxidative damage to endplate chondrocytes in intervertebral disc: implications for the treatment of degenerative lumbar disc. Oxid Med Cell Longev 2017: 4041768, 2017.
10. Ye S, Ju B, Wang H and Lee KB: Bone morphogenetic protein-2 provokes interleukin-18-induced human intervertebral disc degeneration. Bone Joint Res 5: 412-418, 2016.
11. Dai L, Xu M, Wu H, Xue L, Yuan D, Wang Y, Shen Z, Zhao H and Hu M: The functional mechanism of simvastatin in experimental osteoporosis. J Bone Miner Metab 34: 23-32, 2016.
12. Elkadi S, Elsamaligy S, Al-Suwayeh S and Mahmoud H: The development of self-nanoemulsifying liquisolid tablets to improve the dissolution of simvastatin. AAPS PharmSciTech 18: 2586-2597, 2017.

13. Steinbach JM, Seo YE and Saltzman WM: Cell penetrating peptide-modified poly(lactic-co-glycolic acid) nanoparticles with enhanced cell internalization. Acta Biomater 30: 49-61, 2016.
14. Zhang C, An T, Wang D, Wan G, Zhang M, Wang H, Zhang S, Li R, Yang X and Wang Y: Stepwise pH-responsive nanoparticles containing charge-reversible pullulan-based shells and poly(β-amino ester)/poly(lactic-co-glycolic acid) cores as carriers of anticancer drugs for combination therapy on hepatocellular carcinoma. J Control Release 226: 193-204, 2016.
15. Chen J, Xuan J, Gu YT, Shi KS, Xie JJ, Chen JX, Zheng ZM, Chen Y, Chen XB, Wu YS, *et al*: Celastrol reduces IL-1β induced matrix catabolism, oxidative stress and inflammation in human nucleus pulposus cells and attenuates rat intervertebral disc degeneration in vivo. Biomed Pharmacother 91: 208-219, 2017.
16. Liu J, Tao H, Wang H, Dong F, Zhang R, Li J, Ge P, Song P, Zhang H, Xu P, *et al*: Biological behavior of human nucleus pulposus mesenchymal stem cells in response to changes in the acidic environment during intervertebral disc degeneration. Stem Cells Dev 26: 901-911, 2017.
17. Gentile P, Nandagiri VK, Daly J, Chiono V, Mattu C, Tonda-Turo C, Ciardelli G and Ramtoola Z: Localised controlled release of simvastatin from porous chitosan-gelatin scaffolds engrafted with simvastatin loaded PLGA-microparticles for bone tissue engineering application. Mater Sci Eng C 59: 249-257, 2016.
18. Ramazani F, Chen W, van Nostrum CF, Storm G, Kiessling F, Lammers T, Hennink WE and Kok RJ: Strategies for encapsulation of small hydrophilic and amphiphilic drugs in PLGA microspheres: State-of-the-art and challenges. Int J Pharm 499: 358-367, 2016.
19. Terauchi M, Inada T, Tonegawa A, Tamura A, Yamaguchi S, Harada K and Yui N: Supramolecular inclusion complexation of simvastatin with methylated β-cyclodextrins for promoting osteogenic differentiation. Int J Biol Macromol 93: 1492-1498, 2016.
20. Zhang P, Han F, Li Y, Chen J, Chen T, Zhi Y, Jiang J, Lin C, Chen S and Zhao P: Local delivery of controlled-release simvastatin to improve the biocompatibility of polyethylene terephthalate artificial ligaments for reconstruction of the anterior cruciate ligament. Int J Nanomedicine 11: 465-478, 2016.
21. Russell-Puleri S, Dela Paz NG, Adams D, Chattopadhyay M, Cancel L, Ebong E, Orr AW, Frangos JA and Tarbell JM: Fluid shear stress induces upregulation of COX-2 and PGI_2 release in endothelial cells via a pathway involving PECAM-1, PI3K, FAK, and p38. Am J Physiol Heart Circ Physiol 312: H485-H500, 2017.
22. Mayoral-Andrade G, Pérez-Campos-Mayoral L, Majluf-Cruz A, Perez-Campos Mayoral E, Perez Campos Mayoral C, Rocha-Núñez A, Martinez M, Zenteno E, Hernandez-Gonzalez L, López Juan MG, *et al*: Reduced platelet aggregation in women after intercourse: A possible role for the cyclooxygenase pathway. Clin Exp Pharmacol Physiol 44: 847-853, 2017.
23. Fan H, Li M, Yu L, Jin W, Yang J, Zhang Y and Wan H: Effects of Danhong injection on platelet aggregation in hyperlipidemia rats. J Ethnopharmacol 212: 67-73, 2018.
24. Mok FPS, Samartzis D, Karppinen J, Fong DY, Luk KD and Cheung KM: Modic changes of the lumbar spine: Prevalence, risk factors, and association with disc degeneration and low back pain in a large-scale population-based cohort. Spine J 16: 32-41, 2016.
25. Chiang CH, Chu PY, Hou MF and Hung WC: MiR-182 promotes proliferation and invasion and elevates the HIF-1α-VEGF-A axis in breast cancer cells by targeting FBXW7. Am J Cancer Res 6: 1785-1798, 2016.
26. Balamurugan K: HIF-1 at the crossroads of hypoxia, inflammation, and cancer. Int J Cancer 138: 1058-1066, 2016.
27. Huang TH, Chung SY, Chua S, Chai HT, Sheu JJ, Chen YL, Chen CH, Chang HW, Tong MS, Sung PH, *et al*: Effect of early administration of lower dose versus high dose of fresh mitochondria on reducing monocrotaline-induced pulmonary artery hypertension in rat. Am J Transl Res 8: 5151-5168, 2016.
28. Hong F, Wang X and Tu G: Underlying mechanism of effect of Shenfu injection on Buerger's disease model rats. 2011 International Conference on Human Health and Biomedical Engineering IEEE, pp1041-1044, 2011.